Published paper

S. Stipetic, D. Zarko and M. Popescu, "Ultra-fast axial and radial scaling of synchronous permanent magnet machines," in *IET Electric Power Applications*, vol. 10, no. 7, pp. 658-666, 8 2016.

http://dx.doi.org/10.1049/iet-epa.2016.0014

Ultra-Fast Axial and Radial Scaling of Synchronous Permanent Magnet Machines

Stjepan Stipetic[1,*], Damir, Zarko[2], Mircea Popescu[3]

[1]Motor Engineer s.a.r.l, Biviers, France
[2]University of Zagreb Faculty of Electrical Engineering and Computing, Department of Electric Machines, Drives and Automation, Zagreb, Croatia
[3]Motor Design Ltd., Ellesmere, UK
[*]stjepan.stipetic@gmail.com

Abstract: Scaling laws are used when the size of a certain machine design with known performance needs to be adjusted for a new application with known requirements, or when a machine design is geometrically scaled and one needs to determine its performance. Scaling laws derived in this paper allow one to quickly and accurately recalculate parameters of a geometrically scaled permanent magnet machine. They basically consist of two separate important scaling procedures: axial scaling and radial scaling. The third and inevitable scaling procedure is rewinding, which is used to adjust the winding for a required voltage level. Exact but simple analytical equations for the various parameters (torque, power, losses, mass, resistance, inductance, efficiency etc.) of the machine are derived using three independent scaling factors, one for each scaling procedure. Special attention is given to the inclusion of end-winding influence and 3D permanent magnet loss effects. Algorithms for fast determination of winding parameters for a given voltage and fast determination of scaling factors for scaling based on the torque requirement with stack length limitation are presented. All derived scaling equations are numerically validated using two state-of-the-art motor design software packages with automated extraction of parameters based on finite element calculations.

1. Introduction

Scaling (or similitude) laws are popular in physics and engineering and are often used in numerous applications to predict the performance of a new design based on the data from an existing, similar design. In the electromagnetics, new design and similar design will have similar geometry, but in general not the same materials and electromagnetic excitation, both in terms of amplitude and time scale.

Hsieh and Kim [1] presented a detailed derivation of scaling laws for an electromechanical system using the electromagnetic diffusion equation, thermal diffusion equation, momentum equation and kinematic equation along with numerical validation on $\sqrt{2}$ times smaller electromagnetic launcher. Wood [2] was dealing with general scaling laws for electromagnetic systems motivated by thermal stability of magnetic recording systems. From the Landau-Lifshitz-Gilbert equation he concluded that for non-linear ferromagnetic systems there are two independent scaling factors (λ for length, and τ for time). If the time is not scaled, there is only one scaling factor. Kofler *et. al.* [3] explored magnetic field in the end-winding space of a superconducting synchronous machine reduced by scaling laws from [4]. These laws are basically identical to the ones derived in [2].

Bone [5] determined basic scaling laws for induction machines. These laws are not as exact as the ones derived in this paper because the field solutions are changed, but are very valuable as a tool for machine designer. Binns and Shimmin [6] tried to determine basic scaling laws for permanent magnet (PM) machines. Their scaling laws are based on keeping the current density equal for the radially scaled machine which does not keep the same field solution. Gu and Stiebler [7] dealt with scaling laws for switched-reluctance machines; their work was expanded in this paper and applied to PM machines to include the three separate scaling procedures.

The axial scaling (core lengthening) is a known NTC (no tool cost) procedure for induction machines [8, 9] which can be applied also for PM machines, but has a technological limit in terms of stack length. Therefore radial scaling, using a larger frame size, can be utilized in order to achieve larger torque ratings when maximum allowed stack length is reached.

The novel contribution of this paper is a comprehensive definition of analytical scaling laws for PM machines based on rewinding, axial scaling (lengthening or shortening) and proportional radial scaling (increase or reduction in diameter) which include end-winding influence and 3D PM loss effects. These scaling laws are not intended to scale in a large geometrical range due to the natural change of optimal split ratio (the ratio of stator inner and outer diameter) between small, medium and larger-sized machines. As described in this paper, these scaling laws preserve saturation levels in the original and scaled machine, therefore allowing quick and accurate recalculation of parameters of the scaled machine. Presented algorithms can be used to calculate the exact size of a certain machine design with known performance that needs adjustment for a new application and performance.

All derived scaling equations are numerically validated through comparison with the results from two different modern state-of-the-art motor design software packages with background finite element (FE) analysis (SPEED PC-BDC and Motor-CAD). Analytical models for end-windings and magnet loss were thoroughly validated as reported in [10, 11].

2. Motivation

The research related to scaling laws for PM machines begun in order to explore the ability to design the optimal series (set) of the machines by optimizing only one design, so called *referent design*. All of the *particular machines* in the series are considered to be *scaled designs* (scaled from the referent design) and they are calculated by utilizing the scaling laws. In general they have the same rated voltage and rated speed but different torque and power rating. By optimizing only the referent machine and scaling its size to meet the desired power ratings, one can achieve significant savings in the overall time needed to design the series of the machines. Optimality of the referent machine can be preserved to a certain degree which will be described in another paper. Figure 1 shows a series of interior permanent magnet (IPM) machines with rated power between 50 and 150 kW in two standard frame sizes: IEC180 [12] and IEC200. All machines are optimal in relation to the value of maximum torque per rotor volume.

The derivation of scaling relations is based on the requirement that magnetic fields in the scaled model should be the exact image of the fields in the referent model (magnetic flux density is unchanged in all active parts after the scaling procedure) as described in [7]. If the value of the magnetic field is preserved, there is no need for a computationally expensive numerical calculation procedure and the fast analytical recalculation can be utilized. This is the main characteristic of

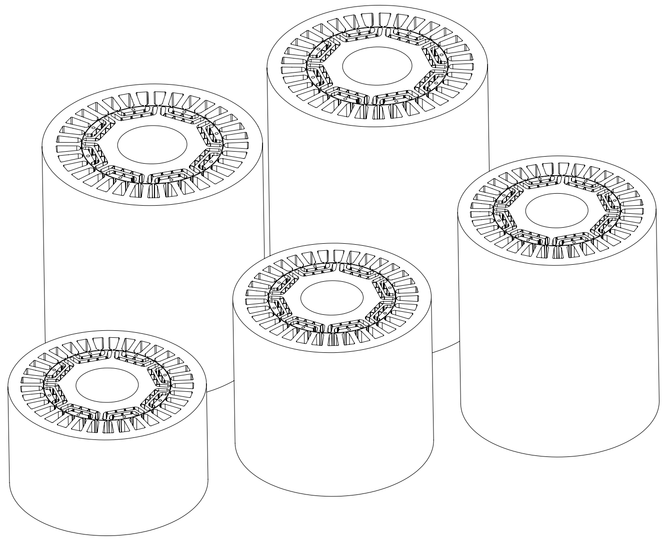

Fig. 1. *Six similar machines: first row 50, 75 and 100 kW in frame size 180, second row: 125 and 150 kW in frame size 200*

all scaling laws derived in this paper. The geometry of the scaled model is similar to the one in the referent model, all the utilized materials and the technology (winding type, slot-fill factor) are the same and the machines operate at the same temperature. The mechanical losses (friction and windage) and AC winding losses are neglected, but can also be scaled according to the principles presented in this paper without the loss of generality.

Although the main limitation of this approach is that magnetic saturation must be preserved in order to avoid numerical recalculation of the scaled machine, there is a strong reason to utilize this approach. By using ultra-fast scaling it is possible to scale any PM machine to have a different length, radial size or rated voltage and quickly calculate its winding parameters and performance characteristics (efficiency map, torque-speed curves). It is also possible to quickly determine the size, the winding features and the characteristics of the similar machine with the desired value of efficiency or shaft torque. The series of machines in Fig. 1 were designed and optimized in a single optimization procedure.

3. Scaling procedures

3.1. Rewinding

Rewinding is a well known procedure related to electrical machines and is normally used to adapt the winding of the machine to the voltage rating of the power supply system. In this case it considers a change of the number of turns per coil (N_c) and the number of parallel paths (a_p) of the referent machine in the same ratio while keeping the slot current density, cross-section geometry and slot fill factor unchanged. In the following text, index 0 denotes that the quantity is related to the referent, initial machine with known parameters, otherwise it is related to the scaled machine.

The referent machine will generally have N_{c0} turns per coil and a_{p0} parallel paths and the rewound (scaled) machine will have N_c turns per coil and a_p parallel paths.

With regard to the initial assumptions ($J = J_0$, $A_{slot} = A_{slot0}$, $k_{Cu} = k_{Cu0}$), one can write

$$I = \frac{a_p}{N_c}\frac{N_{c0}}{a_{p0}} I_0 = \frac{1}{k_W} I_0. \tag{1}$$

where k_W is the rewinding factor.

The rewinding procedure can be independent of any other scaling procedure, but in this paper it is not separable from the axial and radial scaling because the scaled machine must have prescribed voltage rating. Rewinding can be of high importance when determining the optimal winding parameters for a traction drive with prescribed drive cycle [13–15].

3.2. Axial Scaling

Axial scaling stands for the variation of the axial core length by keeping the lamination cross-section preserved. It is considered that the axial length of the stator stack, the rotor stack and the magnets is changed in the same ratio. The stack length of the scaled machine l_{Fe} is determined from

$$l_{Fe} = k_A l_{Fe0}, \tag{2}$$

where k_A is the axial scaling factor and l_{Fe0} is the referent machine stack length. Axially scaled machine is also rewound to have a certain number of turns per coil and parallel paths, both generally not equal to 1, which are chosen to satisfy the prescribed voltage rating.

The slot current density must be preserved in the axial scaling procedure so that magnetic field solutions would stay unchanged. The phase current is therefore only influenced by rewinding

$$I = \frac{1}{k_W} I_0. \tag{3}$$

The change of the axial length does not affect the radial cross-section field solutions but affects magnetic flux, voltage, torque, losses, resistance and inductance. The end winding arrangement and shape is determined only by the lamination cross-section and not by the stack length. There is a technological influence of the number of turns per coil and parallel paths, but it can be neglected in this analysis. It means that all the machines of the same cross section will have equal end winding. Only one part of the scaled machine's flux linkage is affected by the change of the stack length - it is the core part, the one with the subscript co. The end winding part, with the subscript ew, remains unchanged, as shown in equations in section 6.

3.3. Radial Scaling

Radial scaling considers proportional change of all dimensions of the cross-section. It is important to determine under which conditions the magnetic flux densities of the scaled machine are preserved. The Poisson's equation for the referent machine is

$$\frac{\partial}{\partial x}\left(\frac{1}{\mu}\frac{\partial A_z}{\partial x}\right) + \frac{\partial}{\partial y}\left(\frac{1}{\mu}\frac{\partial A_z}{\partial y}\right) = -J_z, \tag{4}$$

and for the scaled machine

$$\frac{\partial}{\partial x'}\left(\frac{1}{\mu'}\frac{\partial A'_z}{\partial x'}\right) + \frac{\partial}{\partial y'}\left(\frac{1}{\mu'}\frac{\partial A'_z}{\partial y'}\right) = -J'_z. \tag{5}$$

Let x and y dimensions be scaled by factor k_R, and slot current density scaled by factor k_J. The terms in the parentheses must be equal for both the scaled and the referent machine in order to preserve the exact same saturation, i.e. the value of μ:

$$\frac{1}{k_R}\frac{\partial}{\partial x}\left(\frac{1}{\mu}\frac{\partial A_z}{\partial x}\right) + \frac{1}{k_R}\frac{\partial}{\partial y}\left(\frac{1}{\mu}\frac{\partial A_z}{\partial y}\right) = -k_J J_z \tag{6}$$

This is accomplished if

$$k_J = \frac{1}{k_R}. \tag{7}$$

All the areas of the cross-section are scaled by factor k_R^2 so the phase current is proportional to the radial scaling factor

$$I \propto J A_{slot} \propto \frac{1}{k_R} J_0 k_R^2 A_{slot0} \propto k_R I_0 \tag{8}$$

which combined with the rewinding gives

$$I = \frac{k_R}{k_W} I_0 \tag{9}$$

Condition in eq. (7) is equivalent to the condition of preserving the specific electric loading (linear current density) which is an obvious consequence of (9). Flux linkage related to the active part (i.e. core) is proportional to the factor k_R due to increase of the stator bore circumference by the factor k_R while the stack length remains unchanged. Flux linked by the end windings is proportional to k_R^2 due to the increase of both circumference and end winding axial length. This is explained in detail in section 4 and the final expressions are given in section 6. Detailed derivation of the expressions for the axial and radial scaling laws can be found in [16] and [17].

4. Scaling of the end region

The end winding region is more difficult to analyse than the core region because the flux paths are situated entirely in the air and its winding structure is often characterized by complex three-dimensional geometry of the coils. An additional difficulty is the effect that adjacent coils and phases have on each other and how their flux is mutually linked in 3D space of the end region.

In the case of axial scaling the end winding geometry does not change since only the core length is altered. In the case of radial scaling it is assumed that end coil size will be scaled by k_R in both axial and circumferential direction. This assumption is drawn from the fact that with increased radial dimensions of the machine more space is required in the axial direction to form the end coil loop as the conductors leave one slot and enter another shifted circumferentially by the coil pitch. Of course, as the radial size of the machine is reduced so is the axial size of the end coil. This leads to a conclusion that length of the conductor in the end coil will be scaled by k_R.

Inductance of the end coil for a referent machine can expressed using a general term

$$L_{0ew} = N_{c0}^2 P_{m0} = N_{c0}^2 \frac{\mu_0 A_{ew0}}{l_{mew0}} \tag{10}$$

where P_{m0} is the equivalent magnetic permeance of the end region, μ_0 is the permeability of vacuum, A_{ew0} is the equivalent area of the end region through which flux lines linked by all the end coils are passing, and l_{mew0} is the equivalent length of the flux lines. Without consideration of rewinding, it follows from this general equation that the end winding inductance of the scaled machine will be

$$L_{ew} = N_{c0}^2 P_m = N_{c0}^2 \frac{\mu_0 k_R^2 A_{0ew}}{k_R l_{mew0}} = k_R L_{ew0} \tag{11}$$

In order to confirm this scaling law, a sophisticated analytical 3D model of the end winding is used which models the end coil as a set of serially connected straight filaments. The end coil self and mutual inductances are calculated by integrating the magnetic vector potential due to the current in one coil along the contour of the other coil using closed form solutions of Neumann integrals. The mutual inductance between any two coils in the end region is calculated by adding the contributions of all possible pairs of filaments in both coils. The method is explained in detail in [11] for the case of a turbogenerator with double-layer involute winding and has been adapted in this paper to the geometry of the two-layer random wound coils of a PM machine. The end winding leakage inductances (L_{ew}) and lengths of the end coils (l_{ew}) have been calculated using this model for radially scaled geometries of the end winding of the IPM motor shown in Fig. 5, with k_R varying from 0.5 to 2.0 and compared in Table 1 with the same values obtained using the defined scaling law. The modelled end windings for k_R equal to 0.5, 1.0 and 2.0 are shown in Fig. 2. The circular lines in the bottom plane show the outlines of the stator inner and outer diameter for all three cases of k_R. For illustration, Fig. 3 shows the photo of the actual end winding of the motor in Fig. 5.

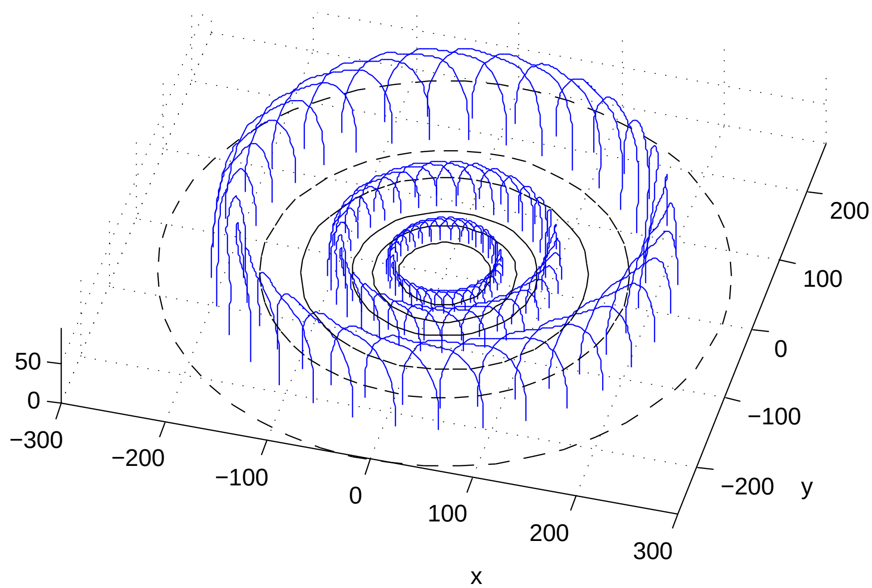

Fig. 2. *Modelled end windings, k_R = 0.5, 1.0, 2.0*

The results in the table indicate that derived scaling law for the end region with almost zero error predicts the scaled length of the end coil conductor in the scaled machine. The error in end winding inductance is lower than 5 % at maximum and minimum scaling factor, which makes the scaling law for the end region reliable for practical applications.

Table 1 Verification of leakage inductance scaling law

	Neumann, [11]		Scaling law		Error, %	
k_R	l_{ew}, mm	L_{ew}, μH	l_{ew}, mm	L_{ew}, μH	l_{ew}	L_{ew}
0.5	133.4	1.62	133.4	1.55	0.03	4.62
0.6	160.2	1.92	160.1	1.86	0.04	3.26
0.7	186.8	2.22	186.8	2.17	0.01	2.22
0.8	213.4	2.51	213.5	2.48	0.05	1.33
0.9	240.2	2.80	240.2	2.79	0.00	0.61
1	266.9	3.10	266.9	3.10	0.00	0.00
1.1	293.6	3.39	293.6	3.41	0.01	0.52
1.2	320.2	3.68	320.3	3.71	0.02	0.98
1.3	347.0	3.97	346.9	4.02	0.02	1.38
1.4	373.6	4.26	373.6	4.33	0.01	1.73
1.5	400.4	4.55	400.3	4.64	0.02	2.05
1.6	427.0	4.84	427.0	4.95	0.00	2.34
1.7	453.6	5.13	453.7	5.26	0.02	2.60
1.8	480.4	5.42	480.4	5.57	0.00	2.83
1.9	506.6	5.71	507.1	5.88	0.09	3.05
2	533.8	6.00	533.8	6.19	0.01	3.25

Fig. 3. *End winding of IPM machine in Fig. 5 without rotor during leakage inductance measurements*

5. Permanent magnet losses and 3D effect

Permanent magnet losses exhibit different behaviour than, for example, iron losses when scaling is considered. Diffusion equation, rather than Poisson's equation must be used and pure volumetric scaling is not applicable. This is the reason for studying them in a separate section of this paper, with axial and radial scaling applied simultaneously. Two-dimensional finite-element analysis (2D FEA) is widely used in electric machine modelling instead of 3D calculations because of their shorter calculation time and simplicity. However, 2D calculations ignore end effects, causing a large error in calculation of eddy currents in permanent magnets of synchronous machines [10]. Additionally, 2D FEA solutions must satisfy the zero net current condition across each conducting region separately, which is not the case in all of the available commercial or free FEA software [18].

According to simplified model of Polinder and Hoeijmakers [19], the eddy-current loss density in a magnet block for 2D case is

$$\frac{P_{mag2D}}{V_m} = \frac{1}{12}\frac{1}{\rho}w_m^2\frac{\partial^2 B}{\partial t^2} \tag{12}$$

and eddy-current loss is then

$$P_{mag2D} = \frac{1}{12}\frac{1}{\rho}w_m^3 h_m L_m\frac{\partial^2 B}{\partial t^2}, \tag{13}$$

where P_{mag2D} is the eddy current loss (W), $V_m = w_m h_m L_m$ is the volume of a PM segment (width*height*length), ρ is the electric resistivity, B is the flux density, and t is the time.

Ruoho *et. al.* [10] developed an analytical model which improves eddy current loss calculation by adjusting the electric resistivity of permanent magnet material according to the magnet dimensions in order to match the actual eddy current path in the magnet block. The 3D/2D correction factor is calculated as follows

$$F = \frac{P_{mag3D}}{P_{mag2D}} = \frac{3}{4}\cdot\frac{L_m^2}{w_m^2 + L_m^2} \tag{14}$$

The eddy current loss calculated in 2D case for radially and axially scaled machine will be

$$\begin{aligned} P_{mag2D} &= \frac{1}{12\rho}w_m^3 h_m L_m\frac{\partial^2 B}{\partial t^2} \\ &= \frac{1}{12\rho}k_R^3 w_{m0}^3 k_R h_{m0} k_A L_{m0}\frac{\partial^2 B_0}{\partial t^2} \\ &= k_R^4 k_A P_{mag2D0} \end{aligned} \tag{15}$$

The eddy current loss with 3D effect included for radially and axially scaled machine will then be

$$\begin{aligned} P_{mag3D} &= \frac{3}{4}\cdot\frac{L_m^2}{w_m^2 + L_m^2}P_{mag2D} \\ &= \frac{3}{4}\frac{k_A^2 L_{m0}^2}{k_R^2 w_{m0}^2 + k_A^2 L_{m0}^2}k_R^4 k_A P_{mag2D0} \end{aligned} \tag{16}$$

This formula also takes axial segmentation into account, but the axially scaled machine must have the same number of segments as the referent machine. The dimensions (w_m, h_m, L_m) and equations (13,14) are related to one magnet segment. Total magnet loss is obtained by summing contributions from all the segments. Circumferential segmentation [20, 21] requires a different correction factor than in (14), but the scaling law itself in (15) is related to 2D loss and any different or new 3D/2D correction factor can be handled in the appropriate manner.

6. Generalized axial and radial scaling laws

6.1. Equations

Equations for generalized scaling laws can be derived using the aforementioned principles. Three key parameters that will alter the frame size, the stack length and the rated voltage are k_R, k_A and k_W respectively. The derived generalized scaling laws therefore include rewinding, axial scaling and radial scaling procedures embedded in equations (18) to (34) which define machine parameters. If the referent machine is excited with the current I_0 and has all the right-hand side parameters indexed with 0 in (18) to (34), then the scaled machine will have all the left-hand side parameters listed in (18) to (34) if excited with current I according to (17). In order to evaluate the effect of a single scaling procedure, one must set all other scaling parameters equal to 1.

$$I = \frac{k_R}{k_W} I_0 \tag{17}$$

$$J = \frac{1}{k_R} J_0 \tag{18}$$

$$\Psi_d = k_W k_R \left(k_A \Psi_{d0co} + k_R \Psi_{0ew}\right) \tag{19}$$

$$\Psi_q = k_W k_R \left(k_A \Psi_{q0co} + k_R \Psi_{0ew}\right) \tag{20}$$

$$T_{em} = k_R^2 k_A T_{em0} \tag{21}$$

$$P_{em} = k_R^2 k_A P_{em0} \tag{22}$$

$$P_{Cu} = k_A P_{Cu0co} + k_R P_{Cu0ew} \tag{23}$$

$$P_{Fe} = k_R^2 k_A P_{Fe0} \tag{24}$$

$$P_{in} = k_R^2 k_A \left(P_{em0} + \frac{1}{k_R^2} P_{Cu0co} + \frac{1}{k_R k_A} P_{Cu0ew}\right) \tag{25}$$

$$P_{mag3D} = \frac{3}{4} k_R^4 k_A \frac{k_A^2 L_{m0}^2}{k_R^2 w_{m0}^2 + k_A^2 L_{m0}^2} P_{mag2D0} \tag{26}$$

$$m_{Cu} = k_R^2 \left(k_A m_{Cu0co} + k_R m_{Cu0ew}\right) \tag{27}$$

$$m_{Fe} = k_R^2 k_A m_{Fe0} \tag{28}$$

$$m_{mag} = k_R^2 k_A m_{m0} \tag{29}$$

$$L_d = k_W^2 \left(k_A L_{d0co} + k_R L_{d0ew}\right) \tag{30}$$

$$L_q = k_W^2 \left(k_A L_{q0co} + k_R L_{q0ew}\right) \tag{31}$$

$$R = \frac{k_W^2}{k_R^2} \left(k_A R_{0co} + k_R R_{0ew}\right) \tag{32}$$

$$V_d = k_W \left\{ \left(\frac{k_A}{k_R} R_{0co} + R_{0ew} \right) I_{d0} - \omega_0 \left[\left(k_R k_A L_{q0co} + k_R^2 L_{q0ew} \right) I_{q0} \right] \right\}, \tag{33}$$

$$V_q = k_W \left\{ \left(\frac{k_A}{k_R} R_{0co} + R_{0ew} \right) I_{q0} + k_R k_A \omega_0 \Psi_{magd0} + \omega_0 \left[\left(k_R k_A L_{d0co} + k_R^2 L_{d0ew} \right) I_{d0} \right] \right\} \tag{34}$$

Cross-saturation parameters Ψ_{magq0}, L_{dq}, L_{qd} are omitted here for the sake of simplicity but they can be scaled appropriately and included in the voltage equations as shown in [16]. In order to reduce the mathematical complexity of the expressions, other important parameters are merely derived from the above mentioned direct scaling expressions

$$P_{shaft} = P_{em} - P_{Fe} - P_{mag3D} \tag{35}$$

$$T_{shaft} = \frac{P_{shaft}}{\omega_0} \tag{36}$$

$$\eta = \frac{P_{shaft}}{P_{in}} \tag{37}$$

$$cos\varphi = \frac{V_d I_d + V_q I_q}{VI} \tag{38}$$

$$V_{ph} = \sqrt{V_d^2 + V_q^2} \tag{39}$$

6.2. *Workflow*

The order of the application of scaling procedures is not relevant for the final result, which means that scaling procedures are independent of each other. The first scaling procedure applied on a referent machine will produce a scaled machine which can be taken as a referent machine for the second scaling procedure and so on. Initial assumptions for a certain procedure (for example for rewinding: $J = J_0$, $A_{slot} = A_{slot0}$, $k_{Cu} = k_{Cu0}$) must be valid only when that procedure is performed. It is important to notice that the slot cross-section will be altered when radial scaling is performed, but it will be exactly the same before and after performing the rewinding and axial scaling. In the same manner, the slot current density must be altered during radial scaling ($J = J_0/k_R$) and kept constant during axial scaling and rewinding. There is no difference if generalized equations shown in section 6.1 or separate equations shown in [16] are used. When separate equations for each scaling procedure are combined one after another, scaling factors are simply being multiplied as shown in (17) to (34).

Nevertheless there is a logical idea behind the order of the application of scaling procedures which can be seen in the algorithms of section 6.3. Both radial and axial scaling alter the torque and the voltage of the machine so one of these two procedures should be selected to be performed initially. Since rewinding does not affect the torque and serves only to match the winding of the machine to the required voltage/current (volt/ampere) rating, it is logical to perform it as a fine tune at the end.

6.3. *Algorithms for automated rewinding and scaling based on the torque requirement*

It is interesting to demonstrate how to quickly calculate the exact number of turns per coil and parallel paths to match the required voltage during the scaling procedure. Due to discrete nature of k_W scaling factor it is not straightforward and easy to calculate the best combination of N_c and a_p. A proposal for automated rewinding algorithm written in Python is

```
def rewind_machine:
 dV_max=1
 for ap_i in possible_a_p:
  for Nc_i in possible_N_c:
   kW = (Nc_i/ap_i)/(Nc_0/ap_0)
   calculate_scaled_Vll()
   dV=abs(Vll-reqV)/reqV
   if Vll<=reqV and dV < dV_max:
    dV_max=dV
    ap=ap_i
    Nc=Nc_i
 kW=(Nc/ap)/(Nc_0/ap_0)
```

The maximum possible number of parallel paths is related to the magnetic symmetry of the machine and it is equal to the periodicity (greatest common divisor of number of slots and poles). Parallel paths are beneficial for the reduction of unbalanced magnetic pull and noise while from manufacturing point of view, higher numbers of parallel paths are often not desirable due to increased copper usage for the terminal connections which leads to the increase of copper loss and end-winding volume. Sometimes it is necessary to match the low voltage/high current demand for a certain machine so that maximum possible a_p is used. Possible number of turns per coil must be greater than one, but there is a certain case-specific limit related to manufacturing due to the change of copper slot fill factor or permissible wire size.

Algorithm searches through all the combinations of possible number of parallel paths (*possible_a_p*) and possible number of turns per coil (*possible_N_c*) to find the best pair *Nc_i* and *ap_i*, which will bring the actual motor terminal line-to-line voltage Vll as close as possible to the inverter line-to-line voltage $reqV$ by minimising the relative voltage difference *dV_max*. High flux, long or high-speed machines use smaller number of turns per coil (sometimes even $N_c = 2$). It is not always possible to match closely the inverter terminal voltage as in the case of the referent machine in Table 3 where terminal voltage is 361 V and the available terminal voltage is 396 V.

Scaling laws are used when a certain design needs to be rescaled for a new application with given required performance and limitations. Since scaling law for electromagnetic torque is volumetric and does not depend on other performance parameters, it is used here as a given required performance parameter along with the required terminal voltage. The limitation parameter in electrical machine scaling is stack length. By lengthening (or shortening) the stack without limit, one can obtain non-technical and non-manufacturable machine sizes. Therefore, there is a limiting value of maximum stack length when increasing the torque and minimum stack length when decreasing the torque. In order to achieve the required torque value, in some cases radial scaling must be utilized as well. A proposal for torque scaling algorithm written in Python is

```
def scale_torque:
 kA=TEM/TEM_0
 kR=1
 if kA>1:
  kA_max=lstk_max/lstk
  if kA>kA_max:
   kR=sqrt(kA/kA_max)
   kA=kA_max
 elif kA<1:
  kAmin=lstk_min/lstk
  if kA<kA_min:
   kR=sqrt(kA/kA_min)
   kA=kA_min
 rewind_machine()
```

The axial scaling factor is determined as a ratio of electromagnetic torque of scaled machine (*TEM*) and referent machine (*TEM0*). If it is greater than one, stack length must be increased. If this increase is greater than the maximum allowed stack length *lstk_max*, axial scaling factor is fixed to the maximum possible value *k_Amax* and radial scaling factor is determined from equations

$$T_{em} = k_R^2 k_{Amax} T_{em0} \tag{40}$$

$$k_R = \sqrt{\frac{k_A}{k_{Amax}}} \tag{41}$$

The opposite case is if axial scaling factor is smaller than one with the limitation of minimum stack length *lstk_min*. Ultimately, an automated rewinding procedure is used to match the required voltage. A similar algorithm can be written if radial scaling is to be primarily used. Maximum and minimum allowed outer diameter is then used as a technological limitation.

6.4. Estimation of the end-winding influence

The scaling laws can be derived without observing the end winding influence separately. Some expressions can be significantly simplified if end winding influence is neglected

$$\Psi_d = k_W k_R k_A \Psi_{d0} \tag{42}$$

$$\Psi_q = k_W k_R k_A \Psi_{q0} \tag{43}$$

$$P_{Cu} = k_A P_{Cu0} \tag{44}$$

$$P_{in} = k_R^2 k_A \left(P_{em0} + \frac{1}{k_R^2} P_{Cu0} \right) \tag{45}$$

$$m_{Cu} = k_R^2 k_A m_{Cu0} \tag{46}$$

$$L_d = k_W^2 k_A L_{d0} \tag{47}$$

$$L_q = k_W^2 k_A L_{q0} \tag{48}$$

$$R = \frac{k_W^2}{k_R^2} k_A R_0 \tag{49}$$

$$V_{ph} = k_W k_R k_A V_{ph0}. \tag{50}$$

Although evaluation time is negligible in both cases, an analysis is performed in order to estimate the end winding influence on some key machine parameters such as terminal voltage, copper loss, total loss and efficiency. The machine used for this analysis is 27s30p SPM torque motor (75 kW, 125 rpm) with relatively low end winding turn length compared to mean turn length (12.3%). Inherently, a fractional slot concentrated winding machine will have short end windings so their influence is low. The plots in Fig. 4 show the difference between using exact and simplified scaling laws vs. axial and radial scaling factor ranging from 0.5 to 2.0. The z-axis shows the value of the difference and the colour shows its absolute value. All plots show relative percentage difference, but only the efficiency plot shows absolute difference because efficiency itself is a relative parameter.

Although analysis like this is example-specific, by observing plots in Fig. 4 it may be concluded without loss of generality:

- difference is equal to 0 for $k_A = k_R$. This can be confirmed by observing equations (30), (31), (47) and (48) which will all have the same form $L = k_W^2 k_A L$,

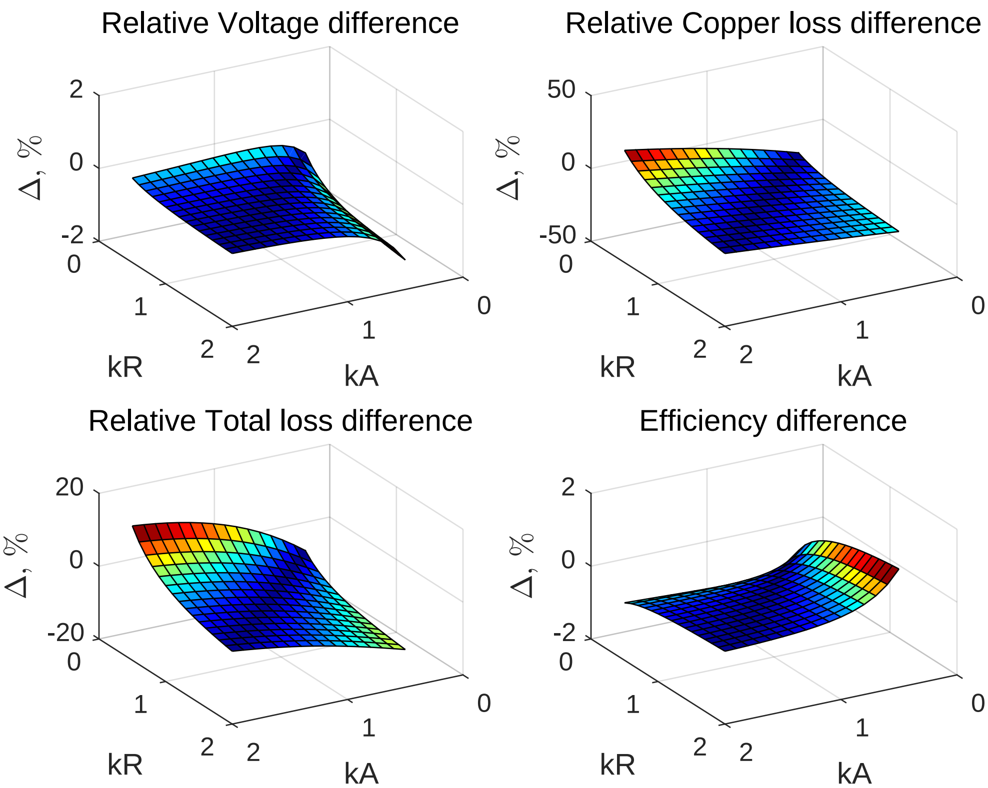

Fig. 4. *Difference in voltage, copper loss, total loss and efficiency when using exact and simplified scaling laws*

- there is no significant end winding influence (less than 1%) on terminal voltage due to small share of flux linkage in the end region compared to the core region,
- there is a significant end winding influence on copper loss (27%, relative), total loss (17%, relative) and efficiency (1.25%, absolute) which confirms the absolute necessity to include the correct end winding resistance scaling in any practical application of scaling laws.

7. Validation

In order to show the correctness of the derived expressions, any general purpose 2D/3D FEA software package can be used. In this case we used specialized motor design (analytical + 2D electromagnetic FEA) packages such as SPEED PC-BDC+PC-FEA, Motor-CAD EMag, MotorSolve etc. which were already thoroughly verified by measurements in the industrial environment. It is important to stress out that scaling laws are valid and can be used for any operating point, not only the rated point. Moreover, it is possible to accurately and quickly rescale the whole efficency map, which will be shown in another paper.

The first example of a referent machine is 110 kW IPM motor (33s8p) which was modelled and calculated using PC-BDC software (analytical + built-in 2D FEA calculation using PC-FEA) by performing static 2D FEA calculations. The results are shown in the 2nd column (original) in table

3 and in Fig. 5. In order to create scaled 63.4 kW machine, the geometry was scaled using the factors $k_R = 0.8$, $k_A = 0.9$, the machine was rewound for the original voltage of 400 V with $k_W = 1.5$ and recalculated in the same software package (results in the 3^{rd} column and in Fig. 5). The results in the 4^{th} (SL = scaling laws) column are obtained using the ultra-fast scaling procedure derived in this paper, the automated rewinding algorithm from section 6.3 and the parameters of the referent 110 kW machine. Permanent magnet loss is negligible. The percentage difference between the parameters recalculated with FE method and the parameters obtained by applying scaling laws is under 1%. The main reason for small differences is the accuracy of FE analysis set to be at least 1% and the uncertainty of the meshing algorithm. The referent and the scaled FEA model consisted of approximately 15500 nodes. The symmetry could not have been exploited due to the slot-pole combination, so all eight poles needed to be modelled.

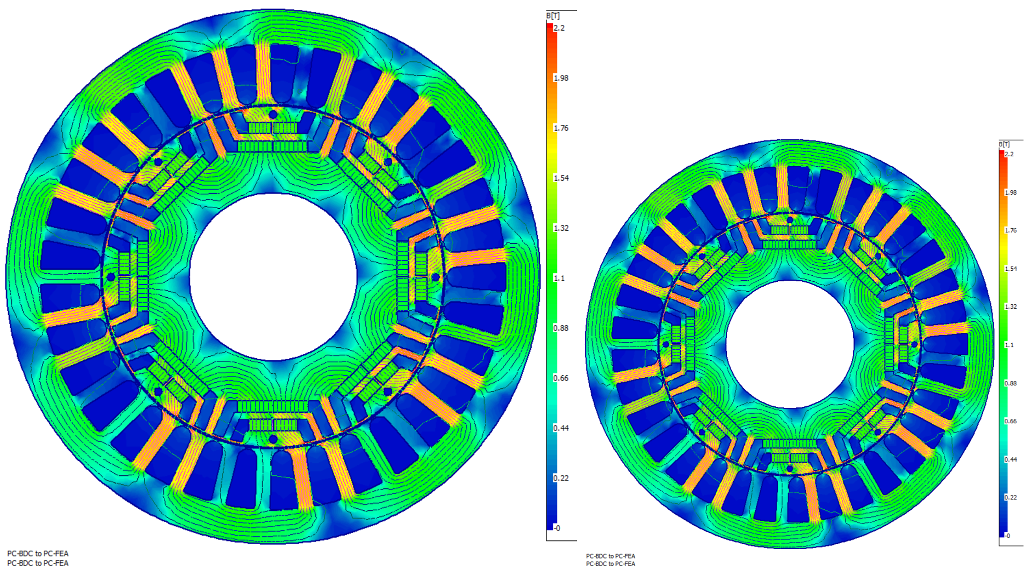

Fig. 5. *Field plot, rated load point for 33s8p IPM: referent design and scaled design, $k_R = 0.8$, $k_A = 0.9$, $k_W = 1.5$*

The second example of a referent machine is the 6.6 kW SPM motor (18s4p) which was modelled and calculated using Motor-CAD EMag software (analytical + built-in 2D FEA calculation) by performing transient 2D FEA calculations. The results are shown in the 2^{nd} column (original) in Table 4 and in Fig. 6. This machine produces electromagnetic torque equal to 21.4 Nm. In order to verify both algorithms in Section 6.3, the referent machine is scaled to produce 30.0 Nm, but with a limit on maximum stack length of 100.0 mm and with required voltage equal to 396.0 V (maximum number of parallel paths equal to 2). The results in the 4^{th} column are obtained by utilizing the torque output scaling algorithm: scaling factors $k_R = 1.124$, $k_A = 1.111$, $k_W = 0.803$. It should be noted that in this case the axial scaling factor was limited by maximum allowed stack length (k_A=100 mm / 90 mm = 1.111), therefore in order to reach the required torque of 30.0 Nm, additional radial scaling by the factor of $k_R = 1.124$ was required. The referent geometry was scaled with obtained scaling factors and recalculated in Motor-CAD EMag. These results are shown in 3^{rd} column and in Fig. 6. The percentage difference between parameters of slow scaling (recalculation with FEA) and ultra-fast scaling (scaling laws) is again negligible. The referent and the scaled FEA model exploited half-symmetry and each model consisted of approximately 5000 nodes.

Furthermore, scaling procedure takes significantly less computational time: it is purely analyti-

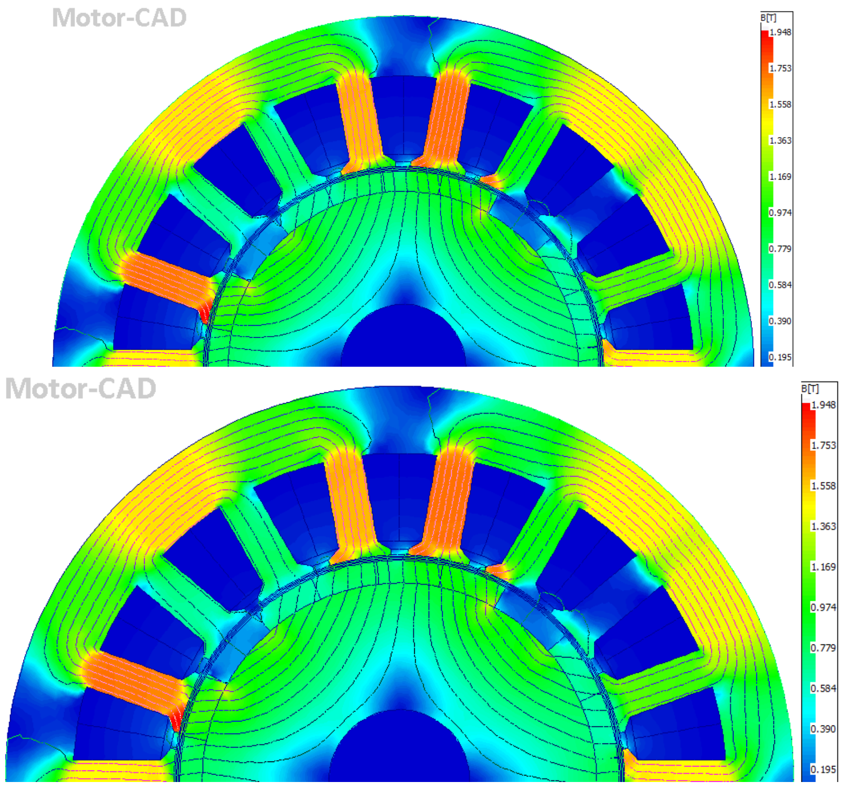

Fig. 6. *Field plot from FE analysis, rated load point for 18s4p SPM: referent design and scaled design,* $k_R = 1.124$, $k_A = 1.111$, $k_W = 0.803$

cal so the results are immediately available. The difference in evaluation time for a computer with Core i5 processor M460, 2.53 GHz, can be observed in Tab. 2. Of course, the evaluation time for FEA calculation depends on the possible symmetry of the machine, mesh density and accuracy used, but this quite large time difference shows the true potential of the scaling laws.

Table 2 Comparison of computational time

Calculation type	Example 1	Example 2
FEA	15 s	23 s
Ultra-fast scaling	10 ms	10 ms

The described ultra-fast scaling method does not aim to show that FEA is not practical or too slow. Time savings reported in Tab. 2 show that repeated use of FEA is not practical when compared to the repeated use of scaling laws. If one should determine scaling factors for required torque with limited stack length and prescribed voltage, without knowing the scaling laws and the algorithm in section 6.3, the process of utilizing FEA calculation would take much more time.

Table 3 IPM, $110\ \mathrm{kW}$ scaled to $63.4\ \mathrm{kW}$, 3000 min^{-1}, 400 V, rated load, phase advance angle $\gamma = 38.3°$, geometry scaled by factors $k_R = 0.8$, $k_A = 0.9$, and machine is rewound for 400 V, $k_W = 1.5$

	FEA ref.	FEA scal.	SL scal.	% diff.
N_c	2	3	3	0.00
a_p	1	1	1	0.00
OD, mm	270.0	216.0	216.0	0.00
l_{stk}, mm	312.0	280.8	280.8	0.00
l_{co}, mm	624.0	561.6	561.6	0.00
l_{ew}, mm	239.0	191.2	191.2	0.00
A_{slot}, mm^2	344.6	220.5	220.5	0.00
J, A/mm^2	5.93	7.42	7.42	0.00
I, A	204.5	109.1	109.1	0.00
T_{shaft}, N m	350.3	201.4	201.8	0.22
T_{em}, N m	358.6	206.1	206.6	0.00
P_{shaft}, kW	110.0	63.4	63.4	0.22
P_{in}, kW	114.4	66.3	66.4	0.19
P_{Cu}, W	1726.6	1506.1	1506.1	0.00
P_{Fe}, W	2570.5	1468.8	1480.6	0.81
η, %	96.22	95.48	95.50	0.03
V_{ph}, V	208.4	226.4	226.5	0.03
V_{LL}, V	361.0	392.2	392.3	0.03
$\cos\varphi$	0.895	0.894	0.896	0.17
L_d, mH	0.37	0.75	0.75	0.06
L_q, mH	0.93	1.88	1.88	0.14
L_{ew}, μH	3.02	5.44	5.44	0.00
R_{ph}, mΩ	13.76	42.20	42.20	0.00
m_{Cu}, kg	17.5	9.7	9.7	0.00
m_{Fe}, kg	79.8	46.0	46.0	0.00
m_{mag}, kg	6.2	3.5	3.5	0.45

Table 4 SPM, 6.6 kW scaled to 9.3 kW, 3000 min^{-1}, 400 V, rated load, geometry scaled by factors $k_R = 1.124$, $k_A = 1.111$, and machine is rewound for 400 V, $k_W = 0.803$

	FEA ref.	FEA scal.	SL scal.	% diff.
N_c	38	61	61	0.00
a_p	1	2	2	0.00
OD, mm	140.0	157.4	157.4	0.00
l_{stk}, mm	90.0	100.0	100.0	0.00
l_{co}, mm	180.0	200.0	200.0	0.00
l_{ew}, mm	107.6	121.0	121.0	0.03
A_{slot}, mm^2	171.4	216.6	216.6	0.00
J, A/mm^2	12.42	11.05	11.05	0.00
I, A	11.2	15.7	15.7	0.00
T_{shaft}, N m	21.0	29.5	29.5	0.10
T_{em}, N m	21.4	30.0	30.0	0.09
P_{shaft}, W	6599.2	9259.9	9265.1	0.02
P_{in}, kW	7207.5	9972.3	9977.8	0.02
P_{Cu}, W	495.5	553.0	553.0	0.01
P_{Fe}, W	109.3	153.5	153.3	0.05
P_{mag3D}, W	3.5	6.1	6.2	1.55
η, %	91.56	92.86	92.86	0.01
V_{ph}, V	228.1	225.7	225.8	0.05
V_{LL}, V	395.0	391.0	391.1	0.05
$\cos\varphi$	0.972	0.971	0.972	0.10
L_d, mH	12.15	8.7	8.7	0.06
L_q, mH	10.86	7.8	7.8	0.07
L_{ew}, µH	221.5	160.5	160.4	0.04
R_{ph}, mΩ	1315.5	748.6	748.4	0.09
m_{Cu}, kg	1.6	2.2	2.2	0.00
m_{Fe}, kg	7.1	9.9	9.9	0.00
m_{mag}, kg	0.5	0.7	0.7	0.00

8. Discussion and Conclusion

Novel ultra-fast scaling laws for PM machines based on three scaling factors are presented and numerically verified. These purely analytical scaling laws are used to obtain the parameters of the scaled machine without the need to recalculate them using the method that was used to calculate the parameters of the referent machine. This is very useful if a computationally expensive numerical method (e.g. FEA), which is very common for synchronous permanent magnet machines, is used.

The scaling method itself is limited by definition: it is based on the preservation of exactly the same magnetic saturation in the referent and scaled machine which leads to two practical limitations. Firstly, all the scaled machines will either have exactly the same or similar (proportionally scaled) lamination design. This can also be understood as a manufacturing benefit because the same lamination stamping tool is used for multiple machines. Secondly, all three scaling procedures imply preservation of the specific electric loading (in A/m). This furthermore implies that during rewinding or axial scaling the current density must be kept unchanged while during radial scaling it must be divided by factor k_R.

The relation of electromagnetic scaling laws with thermal performance adds another important dimension to this problem. In the first approximation if only copper losses are considered, winding temperature rise is proportional to the product of slot current density and specific electric loading. In both radial and axial scaling specific electric loading stays constant. Therefore winding temperature rise is affected only by the change in current density which is reduced if scaling factor is greater than one ($k_R > 1$). In more detail and for the case of radial scaling, iron core loss changes by k_R^2, copper loss is linear with k_R in the end region and unchanged in the core region while cooling surface changes with k_R in the core region and with k_R^2 in the end region. The exact thermal effect depends on the ratio of copper and iron losses, on the thermal properties of the machine and cooling method. However, the relationship between the change of cooling surface and change of losses suggests that no thermal problems will arise. In addition, one must also consider the fact that volume flow of the cooling fan (mounted on the rear for self-ventilated motors) changes with k_R^3 and the pressure changes with k_R^2 so ventilation performance of the motor also changes because it is reasonable to assume that radial and axial size of the cooling fan changes proportionally to radial scaling of the motor laminations. For application of scaling laws in the manufacture of motors or motor series, the thermal aspect must certainly be considered, but that issue exceeds the scope of this paper.

By using ultra-fast scaling it is possible to scale any PM (or synchronous reluctance) machine to have different length, radial size or rated voltage and quickly calculate its winding parameters and performance characteristics (such as efficiency map, torque-speed curves, etc.). Algorithms in section 6.3 can be used to calculate the exact size of a certain machine design with known performance that needs to be adjusted for a new application and performance. The proposed scaling method is also very useful in cases where the optimal design is already achieved but the ratings need to be modified.

Utilization of the scaling laws for PM machines leads to significant time savings when optimized design of a series of machines is performed. While calculating the parameters for every candidate (referent machine) in the optimization procedure, one can at the same time calculate all the parameters for all the machines in the series (axially and/or radially scaled machines). It is then straightforward to calculate the optimization cost function, e.g. the total cost of the material for the series of motors, or the inequality constraint like the minimum allowed efficiency of each machine in the series in various operating points. For each candidate of the optimization procedure and for the optimum solution, exact geometry, winding and accurate performance parameters are immediately known through the scaling laws. The direct usage of FEA to recalculate a single 2D lamination design for different lengths, frame sizes or winding parameters would take too much time for the purpose of evaluating each candidate machine design inside the optimization procedure.

9. Acknowledgment

Stjepan Stipetic is a Marie Curie PostDoc Fellow at Motor Engineer s.a.r.l, Biviers, France on the EU funded Marie Curie ITN project ADvanced Electric Powertrain Technology (ADEPT) project, grant number 607361. This work has also been supported in part by the Croatian Science Foundation under the Project No. IP-11-2013-7801 Advanced Electric Drives for Traction Applications.

10. References

[1] K.-T. Hsieh and B. Kim, "One Kind Of Scaling Relations On Electromechanical Systems," *IEEE Transactions On Magnetics*, vol. 33, no. 1, pp. 240–244, Jan 1997.

[2] R. Wood, "Scaling Magnetic Systems," *IEEE Transactions On Magnetics*, vol. 47, no. 10, pp. 2685–2688, Oct 2011.

[3] H. Kofler, C. Sommerhuber, and F. Zerobin, "The Magnetic Reaction Field In The End Region Of A Synchronous Machine With Superconducting Field Winding," *IEEE Transactions On Magnetics*, vol. 17, no. 5, pp. 1970–1973, Sep 1981.

[4] W. Matthes, "Beitrag Zum Streuende Problem Der Zusatzverluste Durch Magnetische Wechselfelder," *Elektrotechnische Zeitschrift- Ausgabe A*, vol. 90, no. 4, pp. 75–80, 1969.

[5] J. C. H. Bone, "Influence Of Rotor Diameter And Length On The Rating Of Induction Motors," *IEE Journal On Electric Power Applications*, vol. 1, no. 1, pp. 2–6, February 1978.

[6] K. J. Binns and D. W. Shimmin, "The Relationship Between Performance Characteristics And Size Of Permanent Magnet Motors," in *Seventh International Conference On Electrical Machines And Drives, 1995. (Conf. Publ. No. 412)*, Sep 1995, pp. 423–427.

[7] Q. S. Gu and M. Stiebler, "Scaling And Dimensioning Of Switched Reluctance Machines," *European Transactions On Electrical Power*, vol. 7, no. 5, pp. 301–310, 1997.

[8] L. Alberti, N. Bianchi, and S. Bolognani, "Lamination Design Of A Set Of Induction Motors," *Journal Of Electrical Engineering: Theory And Application*, vol. 1, pp. 18–23, 2010.

[9] L. Alberti, N. Bianchi, A. Boglietti, and A. Cavagnino, "Core Axial Lengthening As Effective Solution To Improve The Induction Motor Efficiency Classes," *IEEE Transactions On Industry Applications*, vol. 50, no. 1, pp. 218–225, Jan 2014.

[10] S. Ruoho, T. Santa-Nokki, J. Kolehmainen, and A. Arkkio, "Modeling magnet length in 2-d finite-element analysis of electric machines," *Magnetics, IEEE Transactions on*, vol. 45, no. 8, pp. 3114–3120, Aug 2009.

[11] D. Ban, D. Zarko, and I. Mandic, "Turbogenerator end-winding leakage inductance calculation using a 3-d analytical approach based on the solution of neumann integrals," *Energy Conversion, IEEE Transactions on*, vol. 20, no. 1, pp. 98–105, March 2005.

[12] S. Stipetic, D. Zarko, and M. Kovacic, "Optimised design of permanent magnet assisted synchronous reluctance motor series using combined analytical-finite element analysis based approach," *IET Electric Power Applications*, Accepted for publication, 2016.

[13] M. Barcaro, N. Bianchi, and F. Magnussen, "Permanent-magnet optimization in permanent-magnet-assisted synchronous reluctance motor for a wide constant-power speed range," *Industrial Electronics, IEEE Transactions on*, vol. 59, no. 6, pp. 2495–2502, June 2012.

[14] J. Goss, R. Wrobel, P. Mellor, and D. Staton, "The design of ac permanent magnet motors for electric vehicles: A design methodology," in *IEEE International Electric Machines Drives Conference (IEMDC), 2013*, May 2013, pp. 871–878.

[15] M. Martinovic, D. Zarko, S. Stipetic, T. Jercic, M. Kovacic, Z. Hanic, and D. Staton, "Influence of winding design on thermal dynamics of permanent magnet traction motor," in *International Symposium on Power Electronics, Electrical Drives, Automation and Motion (SPEEDAM), 2014*, June 2014, pp. 397–402.

[16] S. Stipetic, D. Zarko, and M. Popescu, "Scaling laws for synchronous permanent magnet machines," in *Ecological Vehicles and Renewable Energies (EVER), 2015 Tenth International Conference on*, March 2015, pp. 1–7.

[17] D. Zarko and S. Stipetic, "Criteria For Optimal Design Of Interior Permanent Magnet Motor Series," in *XXth International Conference On Electrical Machines (ICEM), 2012*, Sept 2012, pp. 1242–1249.

[18] T. Miller, M. McGilp, and K. Klontz, "Approximate methods for calculating rotor losses in permanent-magnet brushless machines," in *Electric Machines and Drives Conference, 2009. IEMDC '09. IEEE International*, May 2009, pp. 1–8.

[19] H. Polinder and M. Hoeijmakers, "Eddy-current losses in the segmented surface-mounted magnets of a pm machine," *Electric Power Applications, IEE Proceedings -*, vol. 146, no. 3, pp. 261–266, May 1999.

[20] J. Wang, K. Atallah, R. Chin, W. Arshad, and H. Lendenmann, "Rotor eddy-current loss in permanent-magnet brushless ac machines," *Magnetics, IEEE Transactions on*, vol. 46, no. 7, pp. 2701–2707, July 2010.

[21] P. Sergeant and A. Van den Bossche, "Segmentation of magnets to reduce losses in permanent-magnet synchronous machines," *Magnetics, IEEE Transactions on*, vol. 44, no. 11, pp. 4409–4412, Nov 2008.